EPJ Web of Conferences **113**, 01008 (2016)
DOI: 10.1051/epjconf/201611301008

Electromagnetic structure of light nuclei

Saori Pastore[1,2,a]

[1] *Department of Physics and Astronomy, University of South Carolina, Columbia, SC 29208, USA*
[2] *Theoretical Division, Los Alamos National Laboratory, Los Alamos, NM 87545, USA*

Abstract. The present understanding of nuclear electromagnetic properties including electromagnetic moments, form factors and transitions in nuclei with A $\leq$ 10 is reviewed. Emphasis is on calculations based on nuclear Hamiltonians that include two- and three-nucleon realistic potentials, along with one- and two-body electromagnetic currents derived from a chiral effective field theory with pions and nucleons.

1 Introduction

A major goal in nuclear physics is to understand nuclear structure and dynamics in terms of underlying interactions occurring between individual nucleons. Studies grounded on this basic picture of the nucleus are referred to as *ab initio*. An exceptionally powerful tool to asses the validity of our theoretical models is to investigate nuclear electromagnetic (e.m.) observables, such as ground state properties, *e.g.*, e.m. moments and form factors, as well as e.m. reactions, *e.g.*, photon- and electro-induced reactions. In these processes, external e.m. probes interact with the nuclear charge and current distributions with a strength characterized by the fine-structure constant $\alpha \sim 1/137$. The small value of the fine-structure constant allows for a perturbative treatment of the e.m. interaction, while non-perturbative physics pertains only to the nuclear target. For light nuclei, terms that go beyond the leading order contribution in the $Z\alpha$-expansion (where Z is the number of protons) can be safely disregarded, leaving us with relatively simple reaction mechanisms and manageable formal expressions. For example, at leading order, the cross section associated with the inclusive electron-nucleus scattering processes is factorized into the leptonic tensor, which is completely specified by the measured electron's kinematic variables, and the hadronic one associated with the nuclear target, and proportional to matrix elements squared of the nuclear e.m. charge and current operators. A clear connection between measured quantities, *i.e.*, cross sections, and calculated matrix elements is then realized. Experimental data of e.m. observables are, in most cases, known with great accuracy providing us with viable and strong constraints on our models. Likewise, for light nuclei, theoretical calculations are affected by relatively small numerical errors because for these systems the many-body problem can be solved exactly or within controlled approximations. This allows for solid comparisons between experimental data and theoretical predictions.

In Fig. 1, a cartoon picture of the double differential cross section for electron scattering off nuclei is represented. Different values of energy ω transferred to the system, correspond to different excitation energies of the nucleus. By varying ω, we can access the ground state (elastic peak), low-lying

[a] e-mail: saori@lanl.gov

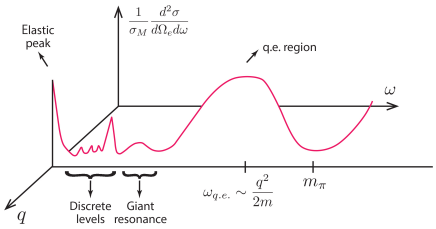

Figure 1. Schematic representation of the double differential cross section for electron scattering off nuclei at fixed value of momentum transfer.

(discrete) nuclear excited states, giant resonance modes, and the quasi-elastic energy region up to the pion-production threshold. For each value of excitation energy ω, one can study the matrix elements' behavior as a function of the momentum $|\mathbf{q}|$ transferred to the nucleus. In particular, by varying $|\mathbf{q}|$ one can explore the e.m. charge and current distributions with a spatial resolution $\propto 1/|\mathbf{q}|$. In this talk, I will focus on *ab initio* calculations of ground state nuclear e.m. properties, that is e.m. moments and elastic form factors, as well as widths of e.m. transitions occurring between low-lying nuclear states. These studies have been recently reported in a topical review on e.m. reactions on light nuclei [1], where more details and references to original articles can be found. Recent developments on theoretical *ab initio* investigations on other very interesting e.m. processes in light nuclei, such as photo-absorption and radiative capture reactions, Compton scattering, sum rules ..., are well represented in this conference, see, *e.g.*, contributions by X. Zhang, J. Dohet-Eraly, H. Griesshammer, M. Miorelli, S. Bacca, N. Barnea, D. Rozpedzik, and A. Lovato in these proceedings.

A theoretical understanding and control of nuclear e.m. structure and dynamics is a necessary prerequisite for studies on weak induced reactions, such as neutrino-nucleus interactions. The experimental data acquisition for this kind of processes is comparatively more involved owing to the tinier cross sections and to the fact that neutrinos are chargeless particles and, thus, they are hard to collimate and detect. An important advance in this direction has recently been carried out by Lovato and collaborators [2], and for a status report on *ab initio* calculations of weak response functions in ^{4}He and ^{12}C I refer to the plenary talk of A. Lovato (the associated contribution can be found in these proceedings). Moreover, a theoretical understanding of the structure and dynamics of light nuclei is a necessary prerequisite for research projects aimed at studying larger nuclear systems. For these reasons, it is imperative to first validate our theoretical understanding of e.m. reactions on light nuclei.

2 Nuclear Hamiltonians and electromagnetic currents

In the *ab initio* framework, the nucleus is described as a system made of A non-relativistic point-like nucleons interacting among each other via many-body forces and its energy is approximated by the following Hamiltonian:

$$H = \sum_i K_i + \sum_{i<j} v_{ij} + \sum_{i<j<k} V_{ijk} \,, \tag{1}$$

where K_i is the non-relativistic single-nucleon kinetic energy, while v_{ij} and V_{ijk} are two-nucleon (NN) and three-nucleon (3N) potentials, respectively. Implicit in the equation above is the assumption that four-nucleon forces and higher terms in the many–body expansion are suppressed. The NN and 3N potentials are phenomenological in nature in that they involve a number of parameters—subsuming

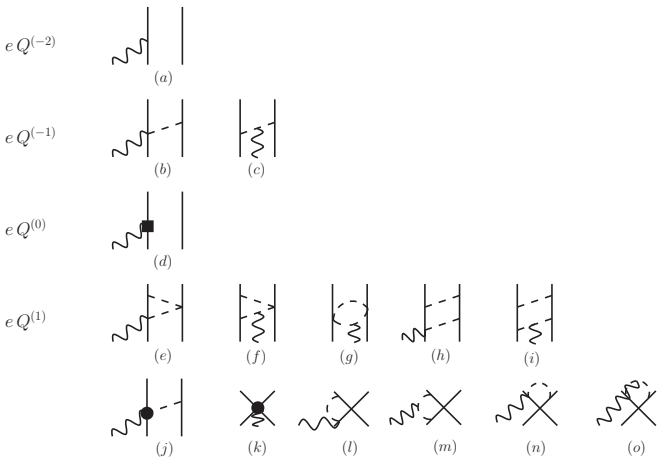

Figure 2. Diagrams illustrating one- and two-body EM currents entering at LO ($e\,Q^{-2}$), NLO ($e\,Q^{-1}$), N2LO ($e\,Q^{0}$), and N3LO ($e\,Q^{1}$). Nucleons, pions, and photons are denoted by solid, dashed, and wavy lines, respectively.

underlying Quantum Chromodynamics (QCD) effects—that are fixed by fitting experimental data. For example, NN potentials are constrained to reproduce a large number of NN scattering data, along with the deuteron binding energy. Nuclear forces belonging to this class of highly accurate nuclear potentials are referred to as 'realistic'. Most realistic potentials describe the long range ($\propto 1/m_\pi$ where m_π is the pion mass) part of the nuclear interaction in terms of one-pion-exchange interaction mechanisms. Different dynamical schemes are implemented to account for intermediate and short range effects, among which multiple-pion-exchange, contact interactions, heavy-meson-exchange, or excitations of nucleons into virtual Δ-isobars. Here, the realistic potentials utilized to solve the Schrödinger equation $H|\Psi\rangle = E|\Psi\rangle$ (where $|\Psi\rangle$ is the nuclear wave function) are the Argonne $v18$ [3] (AV18) NN potential in combination with either the Urbana IX [4] or Illinois-7 [5] 3N potentials, as well as combinations of NN and 3N potentials derived from chiral effective field theory (χEFT)[6–9].

Nuclear charge (ρ) and current ($\mathbf{j}$) operators describe the interactions of nuclei with external e.m. probes. They are also expanded in a series of many-body operators as

$$\begin{aligned} \rho &= \sum_i \rho_i(\mathbf{q}) + \sum_{i<j} \rho_{ij}(\mathbf{q}) + \dots\,, \\ \mathbf{j} &= \sum_i \mathbf{j}_i(\mathbf{q}) + \sum_{i<j} \mathbf{j}_{ij}(\mathbf{q}) + \dots\,, \end{aligned} \tag{2}$$

where $\mathbf{q}$ is the momentum transferred to the nucleus. In Impulse Approximation (IA), that is retaining only one-body operators in the equations above, nuclear e.m. charge and current distributions are simply the sums of those associated with individual protons and neutrons. The non-relativistic charge operator for point-like nucleons is simply the proton charge, while the nucleon current consists of a convection term associated with the current generated by moving protons and a spin-magnetization term associated with the spins of both protons and neutrons. The IA picture of the nucleus is, however, incomplete as it fails to explain, *e.g.*, the measured magnetic moments of light nuclei. Corrections that account for processes in which external e.m. probes couple to pairs of interacting nucleons, described by two-body current operators, need to be incorporated in the theoretical *ab initio* description. Meson-exchange currents (MECs)—postulated in the '40s by Villars [10] and Miyazawa [11]—follow

naturally once meson-exchange mechanism are invoked to describe interactions between individual nucleons. They account for processes in which the external e.m. probe couples with mesons being exchanged between nucleons. The first evidence of meson-exchange effects in light nuclei can be traced back to the 1972 work by Riska and Brown [12], in which MECs were found to provide the missing 10% correction to the IA value necessary to reach agreement between the calculated and the measured cross sections for the radiative capture of proton on neutron at thermal neutron energies. Since then, MECs have evolved into highly sophisticated and accurate currents. In their most recent formulation [13, 14], in order to assure consistency between nuclear forces and e.m. currents, MECs are constructed from realistic NN and 3N potentials so as to satisfy the continuity equation. Addition of these MECs corrections to the IA picture successfully explains a wide number of e.m. nuclear observables in light nuclei [15, 16].

Recent years have witnessed the tremendous development and success of χEFT [17–19] that reinforces and grounds the achievements of conventional theoretical approaches. The relevant degrees of freedom of nuclear physics are bounds states of QCD, *i.e.*, pions, nucleons, and Δ's, ... On this basis, their dynamics is completely determined by that associated with the underlying degrees of freedom of quarks and gluons, that is QCD. However, at low energies, QCD does not have a simple solution because the strong coupling constant becomes too large and perturbative techniques cannot be applied to solve it. χEFT is a low-energy approximation of QCD valid in the energy regime where the typical momenta involved, generically indicated by Q, are such that $Q \ll \Lambda_\chi \sim 1$ GeV, where Λ_χ is the chiral-symmetry breaking scale. χEFT provides us with effective Lagrangians describing the interactions between pions, nucleons, and Δ's that preserve all the symmetries, in particular chiral symmetry, exhibited by the underlying theory of QCD at low-energy. These effective interactions, and the transition amplitudes derived from them, can be expanded in powers of the small expansion parameter Q/Λ_χ, restoring, in practice, the possibility of applying perturbative techniques also in the low-energy regime. The unknown coefficients of this expansion in small momenta—referred to as low-energy constants (LECs)—while being tied to QCD effects and therefore attainable from QCD calculations, are, in practice, fixed by comparison with the experimental data. Due to the chiral expansion, it is then possible to evaluate nuclear observables to any degree ν of desired accuracy, with an associated theoretical error roughly given by $(Q/\Lambda_\chi)^{(\nu+1)}$. This calculational scheme has been widely utilized to study both nuclear forces and nuclear electroweak currents. The many-body operators emerging from direct evaluations of the transitions amplitudes with interactions provided by χEFT Lagrangians involve multiple-pion exchange operators, as well as contact-like interaction terms. Nuclear two– and three–body interactions were first investigated in the late '90s by Ordòñez, Ray, and van Kolck using a χEFT with pions and nucleons [20–22]. Currently, chiral NN (3N) potentials commonly used in *ab initio* calculations include up to next-to-next-to-next-to leading order or N3LO (next-to-next-to leading order or N2LO) corrections in the chiral expansion [6, 7, 23].

Vector e.m. currents have been first derived from a χEFT with pions and nucleons by Park, Min, and Rho in Ref. [24]. The resulting operators account for two-pion exchange terms entering at N3LO in the chiral expansion. These currents have been utilized in a number of so called 'hybrid' calculations[1] of nuclear e.m. observables, including magnetic moments and M1 properties of $A = 2$–3 nuclei and radiative capture cross sections in $A = 2$–4 systems [25–27]. More recently, χEFT e.m. currents and charge have been derived up to one loop contributions included within two different implementations of time ordered perturbation theory: one is by the JLab-Pisa group (see Refs. [28–31]) and the other one is by the Bochum-Bonn group (see Refs. [32, 33]). In this talk, I focus on results obtained using chiral e.m. currents, and compare, where possible, different theoretical evaluations

[1] In this kind of calculations, matrix elements of the chiral e.m. charge and current operators are evaluated in between wave functions obtained from conventional realistic potentials, as opposed to potentials derived consistently from χEFT.

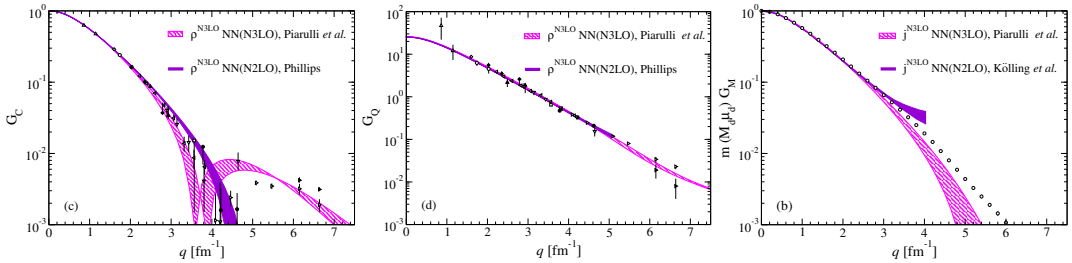

Figure 3. Left: Deuteron charge form factor from Ref. [31] (magenta hatched band) and Ref. [36] (purple solid bands) compared with experimental data (black points). **Middle**: Same as left panel but for deuteron quadrupole form factor. **Right**: Deuteron magnetic form factor from Ref. [31] (magenta hatched band) and Ref. [37] (purple solid band) compared with experimental data (open circles).

against the experimental data. For results based on conventional e.m. MEC currents I refer the reader to the review articles of Refs. [1, 15] and references therein.

Before I proceed presenting applications to e.m. observables, I will briefly describe the e.m. operators as they emerge from a χEFT with pions end nucleons. I will start off with the vector e.m. current which is diagrammatically represented in Fig. 2. The leading order (LO) contribution to the e.m. current illustrated in panel (a) is simply given by the non-relativistic one-body current used in IA calculations, while the N2LO one-body operator of panel (d) is a relativistic correction to the LO IA current. Currents of one- and two-pion range, describing long and intermediate range dynamics, enter at NLO and N3LO—panels (b), (c), (e)—(j). Short-range dynamics is encoded by the contact currents of panel (k). Unknown LECs enter the tree-level diagram of panel (e) and contact currents of panel (k). LECs entering the contact terms are of two kinds, namely minimal and non-minimal. The former enter also the NN chiral potential at NLO, and can then be constrained to NN scattering data; the latter need to be fixed from e.m. experimental data. A common procedure implemented to reduce the number of unknown non-minimal LECs (there are 5 of them) is to impose that the two LECs entering the isovector part of the tree-level current illustrated in panel (e) are in fact saturated by the Δ-couplings entering the Δ transition e.m. current [29, 31]. The remaining three LECs are commonly fixed so as to reproduce the magnetic moments of the deuteron, triton, and ^{3}He [31].

Early investigations on the e.m. charge operator in χEFT have been carried out in Refs. [34–36], and more recently loop corrections have been derived in Ref. [32], and subsequently Ref. [30]. In closing, we note that the structure of the charge operator is quite different from that of the vector e.m. current. Two-body corrections, in this case, are expected to be relatively small. In fact, leading two-body operators of one-pion range are suppressed as they enter at N3LO (as opposed to NLO as seen in the case of the vector currents), while there are no free LECs entering the charge operator up to N4LO [30].

3 Deuteron, ^{3}He and ^{3}H electromagnetic form factors

For A = 2-3 nuclei, theoretical calculations performed by different groups are available, which makes it possible to compare them not only with the experimental data but also between themselves to test the solidity of the *ab initio* prescription. The left and middle panels of Fig. 3, show the deuteron charge and quadrupole form factors, respectively, calculated by Piarulli and collaborators [31] (magenta hatched bands) and Phillips [35, 36] (purple bands). Both calculations are based on chiral NN potentials. In particular, Piarulli *et al.* use wave functions from the chiral NN potential at N3LO [38], while Phillips those from the NN interaction at N2LO [39]. The thickness of the bands represents

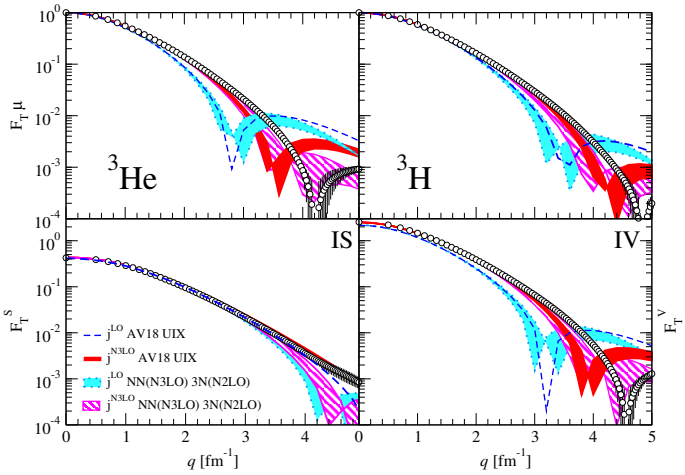

Figure 4. The ^{3}He and ^{3}H magnetic form factors, and their isoscalar and isovector combinations from Ref. [31]. Blue dashed lines (cyan bands) and red (magenta hatched) bands represent calculations based on the AV18+UIX [NN(N3LO)+3N(N2LO)] nuclear Hamiltonians with cumulative χEFT e.m. currents at LO and N3LO, respectively.

the sensitivity of the results to different cutoffs utilized to regularize the divergent behavior at high momenta of the chiral operators' matrix elements [31, 35, 36]. The two calculations very nicely agree with the experimental data for low-value of momentum transferred ($q \simeq 3$ fm^{-1}) and exhibit a similar (small) cutoff dependence. In the case of the charge form factor, as q increases, both theoretical calculations exhibit a more pronounced cutoff dependence, and differ between each other, an indication that this observable is sensitive to the nuclear wave functions utilized in the calculations. In the case of the quadrupole form factor, the agreement with the experimental data is seen up to $q \simeq 6$ fm^{-1}, well beyond the expected regime of validity of the χEFT framework. In the right panel of Fig. 3, we compare the results for the deuteron magnetic form factor obtained by Piarulli *et al.* [31] (hatched magenta band) based on chiral N3LO potential [38] and chiral e.m. currents at N3LO [29], with the fully consistent χEFT calculations by Kölling *et al.* [37] (solid purple band) based on the chiral NN potential at N2LO [39] and chiral e.m. currents at N3LO [32, 33]. The theoretical results are in very good agreement with each other and with the experimental data for values of momentum transferred $q \simeq 3$ fm^{-1}, and present a comparable cutoff dependence.

Form factor calculations of $A = 3$ nuclei have been reported in Ref. [31]. Here, we show results for the trinucleon magnetic form factors obtained utilizing the chiral e.m. currents at N3LO of Refs. [28, 29] and two sets of nuclear Hamiltonians, namely the AV18 [3] NN plus UIX [4] 3N potentials, and the N3LO [38] NN and N2LO [9] 3N potentials. Calculations in IA are given in light blue (based on chiral interactions) and blue (based on conventional interactions), while full calculations that include the complete e.m. current up to N3LO are given in magenta (based on chiral interactions) and red (conventional interactions). In the figure, the top panels show the ^{3}He and ^{3}H magnetic form factors, while the bottom ones show their isoscalar (F_T^S) and isovector (F_T^V) combinations [31]. As is well know from studies based on the conventional approach (see Ref. [15]), two-body e.m. currents are crucial to improve the agreement between the observed positions of the zeros and the predicted ones at LO (or IA). Despite the excellent agreement between theory and experiment for $q \leq 2$ fm^{-1}, the theory underpredicts the data at higher momentum transfers, while the zeros are found at lower values of q than observed. The theoretical description of the first diffraction region is still incomplete.

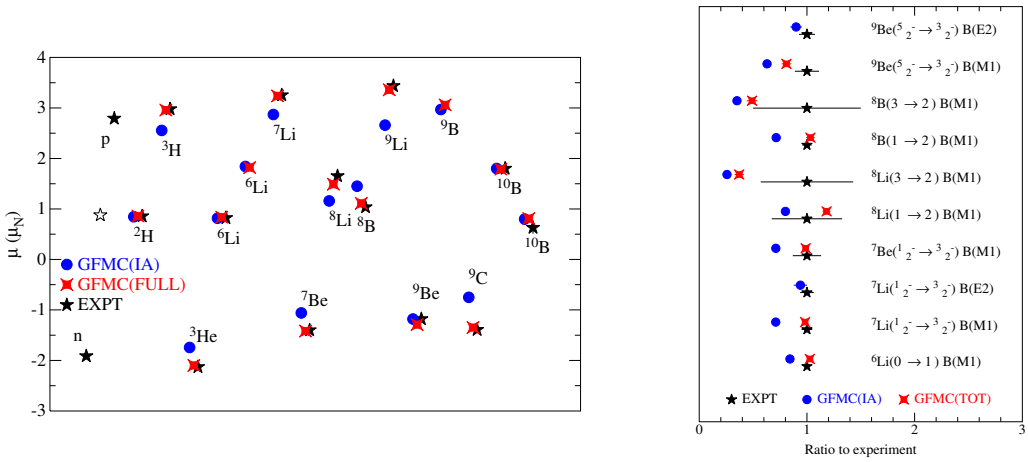

Figure 5. Left: Magnetic moments in nuclear magnetons for $A \leq 10$ nuclei from Ref. [40]. Black stars indicate the experimental values, while blue dots (red diamonds) represent GFMC calculations which include the LO or IA (N3LO) e.m. currents from χEFT. **Right**: Transition widths from Ref. [40] normalized to the experimental values for $A = 6$–9 nuclei. The notation is as in left panel.

4 Magnetic moments and electromagnetic transitions in $A \leq 10$ nuclei

Moving on to larger nuclear systems, we find a number of Greens's Function Monte Carlo calculations [41] based on the AV18 [3] plus IL7 [5] nuclear Hamiltonian that use the chiral e.m. currents up to N3LO from Refs. [28, 29, 31]. Magnetic moments of light nuclei [40] are summarized in the left panel of Fig. 5, where IA results are given by blue dots, while calculations that include the full chiral e.m. current operator are indicated by red diamonds to be compared with the experimental data represented by black stars. First, we note that corrections from two-body currents are found to be small where the IA picture is satisfactory (see, *e.g.*, ^{6}Li, ^{9}Be, ^{10}B), and large where the IA picture is incomplete (see, *e.g.*, ^{7}Li, ^{7}Be, ^{9}C, ^{9}Li). Corrections from two-body components can be as large as 40%, as seen in the case of ^{9}C, and are crucial to reach (or improve) the agreement with the experimental data. It is also interesting to note that two-body effects, while being significant for the ^{9}C and ^{9}Li magnetic moments, are found to be negligible for those of ^{9}Be and ^{9}B. This behavior can be explained considering the dominant spatial symmetries of the nuclear wave functions for these $A = 9$ systems. For example, the dominant spatial symmetry of ^{9}Be (^{9}B) corresponds to an $[\alpha, \alpha, n(p)]$ structure [42]. Therefore, the unpaired nucleon outside the α clusters does not interact with other nucleons. As a consequence, two-body currents, that describe the coupling of external e.m. probes with pair of interacting nucleons, produce a negligible correction. On the other hand, the dominant spatial symmetry of ^{9}C (^{9}Li) corresponds to an [α, ^{3}He (^{3}H), pp (nn)] structure, and two-body correlations contribute in both the trinucleon clusters and in between the trinucleon clusters and the valence pp (nn) pair, resulting in a large two-body current contribution.

GFMC calculations of selected E2 and M1 transitions in low-lying nuclear states [40] are summarized in the right panel of Fig. 5. Predictions in IA are represented by blue dots, while those obtained with the full chiral e.m. current operator are represented by red diamonds. Calculations for E2 transitions implicitly include the effect of two-body currents via the Siegert theorem, where the charge density is used in IA. Also for these observables the effect of two-body e.m. currents can be large, and for cases in which the experimental errors are relatively small, *e.g.*, $^{7}\mathrm{Li}(1/2^- \rightarrow 3/2^-)$, $^{8}\mathrm{B}(1^+ \rightarrow 2^+)$, it is found that their inclusion leads to agreement with the experimental data. This scheme has been

most recently utilized to study e.m. (both E2 and M1) transitions occurring in ^{8}Be [43, 44]. It is found that the agreement between the calculated and the experimental M1 widths is not satisfactory. Nevertheless, chiral two-body e.m. currents provide corrections at the 20%-30% level, which, in all but one case, improves the IA values. It is possible that the systematic underprediction of these observables is due to a poor knowledge of the small components entering the calculated GFMC nuclear wave functions [44].

5 Summary and outlook

In this talk, I presented an overview on the present status of *ab initio* calculations of e.m. observables, including e.m. moments and form factors, as well as e.m. transitions in light nuclei. The emphasis was on calculations that account for NN and 3N potentials in the nuclear Hamiltonians utilized to generate the wave functions, and one- and two-body e.m. current operators. I focused on results that account for two-body operators that have been derived from a χEFT formulation with pions and nucleons, including up to corrections of two-pion range. The *ab initio* prescription is extremely successful in explaining the experimental data, provided that many-body effects in both the e.m. currents and nuclear Hamiltonians are accounted for. χEFT based calculations of $A = 2$ and 3 nuclei e.m. form factors [31] nicely agree with the experimental data in the low-energy regime of applicability of χEFTs, with two-body corrections in the e.m. currents playing an important role in improving the agreement between the calculated and the experimental values of the trinucleon magnetic form factors. E.m. two-body current operators provide a 40% correction in the calculated magnetic moment of ^{9}C [40], and corrections at the 20%-30% level in M1 transitions occurring in ^{8}Be [44]. There are many interesting e.m. observables that can be accessed within this formalism. For example, few (or no) *ab initio* calculations of e.m. (charge and magnetic) form factors in $A > 4$ nuclei currently exist [1], and it would be interesting to perform them to have a deeper insight on nuclear e.m. structures. A complete microscopic profile of nuclei includes also studies of e.m. reactions such as radiative captures and photonuclear reactions. From the theoretical point of view, *i*) the construction of chiral potentials compatible with Quantum Monte Carlo computational calculations [45], opens up the possibility of performing consistent Quantum Monte Carlo calculations that use chiral potentials and chiral currents; *ii*) the construction of the chiral NN potential with the explicit inclusion of Δ-excitation [46], allows study of the effects of Δ-isobars in chiral two-body e.m. current operators [28]. Weak processes are also being vigorously studied within the χEFT formulation. Among these studies are the derivation of the axial two-body current operator up to one-loop [47], as well as the construction of two-body operators entering pion-production reactions induced by neutrino scattering off nuclei (see contributions by F. Myhrer in this proceedings).

Acknowledgements

This work was supported by the National Science Foundation, grant No. PHY-1068305. I am grateful and owe sincere thanks to R. Schiavilla, R.B. Wiringa, Steven Pieper, L. Girlanda, M. Piarulli, M. Viviani, L.E. Marcucci, A. Kievsky, and S. Bacca.

References

[1] S. Bacca, S. Pastore, J. Phys. **G41**, 123002 (2014), 1407.3490

[2] A. Lovato, S. Gandolfi, J. Carlson, S.C. Pieper, R. Schiavilla, Phys. Rev. Lett. **112**, 182502 (2014)

[3] R.B. Wiringa, V.G.J. Stoks, R. Schiavilla, Phys. Rev. C **51**, 38 (1995)
[4] B. Pudliner, V. Pandharipande, J. Carlson, R.B. Wiringa, Phys. Rev. Lett. **74**, 4396 (1995)
[5] S.C. Pieper, AIP Conference Proceedings **1011**, 143 (2008)
[6] R. Machleidt, D. Entem, Physics Reports **503**, 1 (2011), and references therein.
[7] E. Epelbaum, U.G. Meißner, Ann. Rev. Nucl. Part. Sci. **62**, 159 (2012), and references therein.
[8] D. Gazit, S. Quaglioni, P. Navrátil, Phys. Rev. Lett. **103**, 102502 (2009)
[9] P. Navrátil, Few-Body Systems **41**, 117 (2007)
[10] F. Villars, Phys. Rev. **72**, 256 (1947)
[11] H. Miyazawa, Progress of Theoretical Physics **6**, 801 (1951)
[12] D. Riska, G. Brown, Phys. Lett. B **38**, 193 (1972)
[13] L.E. Marcucci, M. Viviani, R. Schiavilla, A. Kievsky, S. Rosati, Phys. Rev. C **72**, 014001 (2005)
[14] L.E. Marcucci, M. Pervin, S.C. Pieper, R. Schiavilla, R.B. Wiringa, Phys. Rev. C **78**, 065501 (2008)
[15] J. Carlson, R. Schiavilla, Rev. Mod. Phys. **70**, 743 (1998), and references therein.
[16] A. Lovato, S. Gandolfi, R. Butler, J. Carlson, E. Lusk et al., Phys. Rev. Lett. **111**, 092501 (2013)
[17] S. Weinberg, Phys. Lett. B **251**, 288 (1990)
[18] S. Weinberg, Nucl. Phys. B **363**, 3 (1991)
[19] S. Weinberg, Phys. Lett. B **295**, 114 (1992)
[20] U. van Kolck, Phys. Rev. C **49**, 2932 (1994)
[21] C. Ordóñez, U. van Kolck, Phys. Lett. B **291**, 459 (1992)
[22] C. Ordóñez, L. Ray, U. van Kolck, Phys. Rev. C **53**, 2086 (1996)
[23] E. Epelbaum, H.W. Hammer, U.G. Meißner, Rev. Mod. Phys. **81**, 1773 (2009), and references therein.
[24] T.S. Park, D.P. Min, M. Rho, Nucl. Phys. A **596**, 515 (1996)
[25] Y.H. Song, R. Lazauskas, T.S. Park, D.P. Min, Phys. Lett. B **656**, 174 (2007)
[26] Y.H. Song, R. Lazauskas, T.S. Park, Phys. Rev. C **79**, 064002 (2009)
[27] R. Lazauskas, Y.H. Song, T.S. Park, Phys. Rev. **C83**, 034006 (2011)
[28] S. Pastore, R. Schiavilla, J.L. Goity, Phys. Rev. C **78**, 064002 (2008)
[29] S. Pastore, L. Girlanda, R. Schiavilla, M. Viviani, R.B. Wiringa, Phys. Rev. C **80**, 034004 (2009)
[30] S. Pastore, L. Girlanda, R. Schiavilla, M. Viviani, Phys. Rev. C **84**, 024001 (2011)
[31] M. Piarulli, L. Girlanda, L. Marcucci, S. Pastore, R. Schiavilla et al., Phys. Rev. **C87**, 014006 (2013)
[32] S. Kölling, E. Epelbaum, H. Krebs, U.G. Meißner, Phys. Rev. C **80**, 045502 (2009)
[33] S. Kölling, E. Epelbaum, H. Krebs, U.G. Meißner, Phys. Rev. C **84**, 054008 (2011)
[34] M. Walzl, U.G. Meißner, Phys. Lett. B **513**, 37 (2001)
[35] D.R. Phillips, Phys. Lett. B **567**, 12 (2003)
[36] D.R. Phillips, J. Phys. **G34**, 365 (2007)
[37] S. Kolling, E. Epelbaum, D. Phillips, Phys. Rev. **C86**, 047001 (2012)
[38] D.R. Entem, R. Machleidt, Phys. Rev. C **68**, 041001 (2003)
[39] E. Epelbaum, W. Glöckle, U.G. Meißner, Nucl. Phys. A **747**, 362 (2005)
[40] S. Pastore, S.C. Pieper, R. Schiavilla, R. Wiringa, Phys. Rev. **C87**, 035503 (2013)
[41] J. Carlson, S. Gandolfi, F. Pederiva, S.C. Pieper, R. Schiavilla, K.E. Schmidt, R.B. Wiringa (2014), 1412.3081
[42] R.B. Wiringa, Phys. Rev. **C73**, 034317 (2006)

[43] V. Datar, D. Chakrabarty, S. Kumar, V. Nanal, S. Pastore et al., Phys. Rev. Lett. **111**, 062502 (2013)
[44] S. Pastore, R.B. Wiringa, S.C. Pieper, R. Schiavilla, Phys. Rev. C **90**, 024321 (2014)
[45] J.E. Lynn, J. Carlson, E. Epelbaum, S. Gandolfi, A. Gezerlis, A. Schwenk, Phys. Rev. Lett. **113**, 192501 (2014), 1406.2787
[46] M. Piarulli, L. Girlanda, R. Schiavilla, R. Navarro Pérez, J.E. Amaro, E. Ruiz Arriola, Phys. Rev. **C91**, 024003 (2015), 1412.6446
[47] A. Baroni, L. Girlanda, S. Pastore, R. Schiavilla, M. Viviani (2015), arXiv:1509.07039